Effect of Varying Austenitizing Temperatures on Carbide Reduction and Mechanical Properties of Annealed Thin Wall Ductile Iron

[1]Ezenwanyi F. Ochulor, [2]Samson O. Adeosun, [3]Ajibola I. Ashade, and [4] Ademola J. Kareem
[1,2,3,4]Department of Metallurgical and Materials Engineering, University of Lagos, Akoka, Nigeria
eochulor@unilag.edu.ng|sadeosun@unilag.edu.ng|ikeoluwaashadeo4@gmail.com|joe.loe944@gmail.com

Received: 09-APRIL-2026; Reviewed: 25-JUNE-2026; Accepted: 10-AUGUST-2026
https://dx.doi.org/10.46792/fuoyejet.v11i3.1559

ORIGINAL RESEARCH

Abstract— A major design option in automotive parts is to use lightweight materials with exceptional mechanical properties for energy saving requirement. Ductile Irons (DIs) are a viable option due to their good castability, machinability, mechanical, fatigue properties and wear resistance. Despite these, size reduction poses a challenge on mechanical properties and large volumes of carbide precipitations become evident in the microstructure. In this study, 3- and 4-mm thin wall ductile iron (TWDI) green sand mould cast samples, with carbide precipitates were subjected to a full annealing treatment using varying austenitizating temperatures of 905, 920 and 935 °C. Microstructure and mechanical properties were analyzed using scanning electron microscopy (SEM), optical microscopy (OM), and X-ray diffractometry (XRD), tensile tests and Vickers hardness. Microstructures of the heat-treated samples showed decline in carbide precipitation in relation to the cast samples. It was noticed that varying austenitization temperatures affected reduction of carbide precipitations significantly. Hardness decreased from 290.9 Hv and 289.95 Hv for as cast samples to 277.2 Hv and 273.9 Hv for 935 °C austenitized samples for 3- and 4-mm thickness samples respectively, the same trend was observed for the tensile strength whereas a progressive increase in ductility was noticed from 4.3 and 4.15 % for as cast samples to 8.3 % and 8.5 % elongation for 935 °C austenitized 3- and 4-mm samples respectively. Carbide peaks reduced with increase in austenitization temperature. The study showed carbide phases that were precipitated during the casting stage could be reduced considerably by using austenitizing temperature of 935 °C.

Keywords— Austenitizing temperature, carbide precipitates, graphite nodules, microstructure, properties,.

1 INTRODUCTION

As cast thin wall ductile iron's (TWDI) properties are challenged by high solidification rate which leads to precipitation of carbides in their microstructure. TWDIs are thin section profiles of Ductile Iron (DI) with thickness that are less than 5mm (Caldera et al., 2007). TWDIs in relation to other ferrous alloys are attractive due to good castability, machinability, mechanical, fatigue properties and wear resistance. Also, as a result of their high strength to weight ratio they offer better mechanical property advantages. These attributes have made them an attractive option for Automotive part production. Some of these parts where TWDIs are adopted are: connecting rods, control arms, wheel rims and exhaust manifolds (Fras et al., 2013). Also, these lightweight parts offer energy saving advantage considering current high energy cost in Nigeria and the world at large. When considering the metallurgy of TWDIs, faster cooling rates favor the precipitation of eutectic carbides whereas slower cooling favors graphite phase nucleation, due to thickness reduction, this challenge is inevitable when casting TWDIs. Carbide phases in TWDIs are shown in Figure 1a, whereas graphite spheroids are shown in Figure 1b. The white areas in Figure 1a shows M_3C carbides which were caused by the eutectic reaction L → austenite (γ) + M_3C. There are also the Ledeburitic carbide types, which are usually present in the microstructure of TWDIs due of the rapid solidification rate induced by reduction in thickness

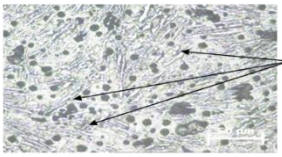

Fig. 1a. Carbide ppt *(Ochulor et al., 2019)*

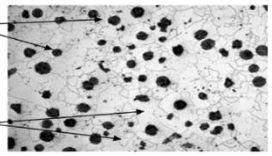

Fig. 1b. Graphite nodules *(Mourad et al., 2015)*

(Giacopini et al, 2003). Casting TWDI sections presents the challenge of large volumes of carbide phases in the as-cast microstructure (Bockus et al., 2008). Over the last two decades attempts have been made by many researchers to eliminate these carbides in the microstructure of TWDIs as they impact negatively on mechanical properties and also cause rejects in as cast TWDIs, some notable ones in literature are highlighted below.

The chemical composition of charge materials is germane, in Riebisch et al. (2020), the researchers investigated some elements such as Chromium, Manganese, Molybdenum, Niobium and Vanadium which are called carbide promoting elements and their impact on graphite morphology, pearlite and carbide fractions in high-silicon DIs with Silicon of 3.8 wt.%. They observed that these elements impacted negatively on nodular graphite nucleation and growth, however they promoted carbide and pearlite phase formation.

Sheikh (2008) adopted the addition of sulphur in the charge material to tackle the issue of carbide precipitation. To get rid of the carbides, the researcher prepared seven melts with different temperatures and compositions. Chemical analyses carried out revealed that high purity of the charge having sulphur that is less than 0.008 wt. %, caused carbide precipitation. The researcher concluded that to remove the carbides from the as cast microstructure, sulphur should be added to the charge materials. Choi et al. (2004) investigated the impact of rare earths (RE) on microstructural evolution

Corresponding Author:
Section D- MATERIALS & METALLURGICAL/CHEMICAL ENGINEERING & RELATED SCIENCES
Can be cited as:
Ochulor E. F., Adeosun S. O., Ashade A. I., and Kareem A. J. (2026). Effect of Varying Austenitizing Temperatures on Carbide Reduction and Mechanical Properties of Annealed Thin Wall Ductile Iron. FUOYE Journal of Engineering and Technology (FUOYE**JET), 11(3),508-513.**
https://dx.doi.org/10.46792/fuoyejet.v11i3.1559

© 2026 The Author(s). Published by Faculty of Engineering, Federal University Oye-Ekiti.
This is an open access article under the CC BY NC license. (https://creativecommons.org/licenses/by-nc/4.0/)

and properties of TWDI castings, they concluded that 2 mm thick samples with varied RE contents showed homogenous graphite nodule distribution, in spite of carbide precipitate formation in all samples, the formation of these carbide phases were less in the samples containing more RE, consequently this enabled more graphite formation. Also, another strategy usually adopted is the alteration of the thermal properties of the molding material to reduce solidification rate of the casting consequently reducing carbide precipitation. Ochulor et al. (2018) adopted this strategy by adding rice husk ash (RHA) to moulding mix in order to modify thermal properties of the molding sand. The moulding mix obtained showed a decline in thermal conductivity consequently impeding carbide precipitation. The same approach was also used in Gorny and Tyrała (2013), where an insulating mould material was adopted consequently lowering the cooling rate of TWDI cast samples. During solidification of TWDIs, since competition takes place between graphite and carbide for carbon contained in molten metal, formation of more eutectic carbides will definitely affect the volume of graphite that can be nucleated (Davies 1996). Berdin et al. (2001) also emphasized on the need to minimize the levels of carbide forming elements in the melt, as carbides will be compete with graphite nucleation in the microstructure.

The challenge of carbide precipitation in TWDIs has made heat treatment an important tool for carbide precipitate reduction or elimination. In Sulamet-Ariobimo et al. (2020), connecting rod TWDI samples were subjected to austempering treatment. The temperature of austenitization was 960˚C with various soaking times and austempering temperature of 350˚C and 35 minutes isothermal treatment. A fluidized bed furnace was adopted for the process. The connecting rods was then subjected to micrstructural examination, tensile and compression tests. The researchers observed that austenitizing time was important for producing thin wall austempered ductile iron (TWADI) since the austenitizing time was responsible for the ausferrite phase nucleation. Also heat treatment could be adopted to improve mechanical properties of as cast DI parts, for example, the study conducted in Adebayo and Oyetunji (2017), where the researchers produced DI from waste sleeve scraps for automotive applications, heat treatment can be adopted to improve the properties of the specimens. In the aforementioned researches, the approach was mainly to modify either the chemical composition of the TWDI melt or the thermal characteristics of the moulding sand, however in this study as cast TWDI samples with carbide precipitates in their microstructure, instead of being considered as rejects were subjected to annealing heat treatment process. This was done by adopting varying austenitizing temperatures in order to investigate the impact of these temperatures on carbide reduction or elimination.

2 METHODOLOGY

2.1 MATERIALS

Charge materials for casting the DI sample for annealing treatment were sourced at Nigerian Machine Tools Limited, Oshogbo, Osun State and consisted of ductile iron returns, ferro-silicon magnesium (FeSiMg) alloy, ferro-silicon (FeSi) alloy and graphite coke. The chemical composition of the ferro silicon (FeSi) alloy inoculant, graphite coke and ferro silicon magnesium (FeSiMg) alloy adopted for casting the DI samples are shown Tables 1, 2 and 3 respectively. Inoculation and magnesium treatments were done using FeSi and FeSiMg ferro alloys respectively. Consumables for Metallography consisted of emery papers and polishing cloth, etching reagent. The equipment and apparatus adopted were Nikon eclipse ME600 metallurgical microscope, pyrometer, heat treatment furnace, optical spectrometer, foundry tongs, hand gloves, polishing machine, angle grinder and portable hacksaw, all located at the Metallurgical and Materials laboratory, University of Lagos, Akoka. The mould was produced according to the requirements as outlined in ASTM E2349-19 procedures for standard mould making. The mould consisted of bentonite, silica sand, water and additives (coal dust and starch). Two wooden rectangular patterns of dimensions 300 x 300 mm for length and breadth with thickness of 3 and 4 mm were adopted for mould making. The moulds were prepared without the use of any mould insulating material as done in Ochulor et al. (2018) and Gorny et al. (2013).

Table 1. Ferrosilicon (FeSi) alloy

Element	Silicon	Aluminum	Carbon	Sulphur	Phosphorus	Iron
Composition (wt.%)	70	0.31	0.0031	0.001	0.001	29.69

Table 2. Graphite coke

Element	Carbon	Ash	Sulphur	Volatile matter	Moisture
Composition (wt.%)	72	27.5	0.2	<0.3	0.1

Table 3. Ferrosilicon magnesium (FeSiMg) alloy

Element	Magnesium	Silicon	Calcium	Aluminum	Rare Earths	Iron
Composition (wt.%)	7.5	44.7	2.02	<0.7	0.8	44.27

2.2 PREPARATION OF TWDI SAMPLES

Melting took place in a 2000 kg Induction furnace, model 13690/1954 Inductotherm in Nigeria Machine Tools Osogbo, tapping of the melt was done at 1480 ^{o}C, after which the melt was discharged into the preheated treatment ladle. Two stage inoculation treatment was done for optimum graphite precipitation, firstly the FeSi inoculants were added to the melt in the pouring ladle after transfer from the treatment ladle. The second inoculation was done while pouring into the moulds using a perforated pipe that delivered powdered FeSi into the melt stream. Magnesium treatment was performed via the sandwich process in the ladle using FeSiMg alloy granules covered in mild steel chips. The moulds were then left to cool after pouring, fettling was later done to isolate the thin wall samples.

2.3 HEAT TREAMENT

The 3- and 4-mm samples were machined for mechanical property tests namely tensile and hardness and microstructural analysis. The Equipment adopted were optical microscope, scanning electron microscope and X-

© 2026 The Author(s). Published by Faculty of Engineering, Federal University Oye-Ekiti.
This is an open access article under the CC BY NC license. (https://creativecommons.org/licenses/by-nc/4.0/)

http://dx.doi.org/10.46792/fuoyejet.v11i3.1559 engineering.fuoye.edu.ng/journal

ray diffractometer. Machined samples for heat treatment were then placed in the furnace and heated to three austenization temperatures of 905 °C, 920 °C and 935 °C for the austenitization treatments prior to oven cooling to room temperature. The soaking time adopted was 10 mins for all the samples. Samples were charged into the furnace by putting two thicknesses (3 mm and 4 mm) for the same heat treatment cycle at the same time. After the soaking time of 10 minutes is achieved, the samples were cooled in the furnace to room temperature.

2.4 MICROSTRUCTURAL CHARACTERISATION

All the samples were machined according to specifications in ASTM E3-11(2017) standard for the preparation of metallographic samples. Cutting, grinding and polishing of samples were done. Using 2% nital solution as the etchant, etching was done to reveal the microstruture under the microscope using standard specifications as outlined in ASTM E407-15. Viewing of the samples was carried out using CETI Optical Metallurgical Microscope (model no 0703552). The optical micrographs were analysed using specifications as outlined in ASTM A247-19. The nodularity estimation was carried out in accordance to Equation (1). In the SEM analysis, the samples were placed in the viewing chamber of the SEM machine.

Nodule Count (graphite nodules/mm^2) is the quantity of nodules per square millimetre on a polished surface examined at X100 magnification.

$$\text{Nodularity } \% = \frac{Area\ (number) of\ acceptible\ particles}{Area\ (number) of\ all\ particles} \text{ X } 100 \qquad (1)$$

2.5 TENSILE TEST

Tensile tests were conducted in accordance with ASTM E8/E8M-16 standard specifications using a computer controlled 100 kN capacity Universal Instron Machine model 3369. Yield and ultimate tensile stress were determined as well as the elongation from the computer software as a graph of stress/strain is plotted, this was done for the DI control 3- and 4-mm samples prior to heat treatment and after heat treatment of the 3- and 4-mm samples. The schematic representation of the tensile test sample as shown in Figure 2. Two test pieces were prepared for tensile test, after which the average was taken for the parameter under investigation.

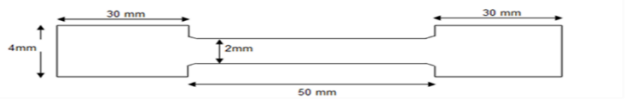

Fig. 2. Dimension of tensile test piece

2.6 HARDNESS TEST

Vickers hardness of the samples before heat treatment and after were evaluated using the Vickers micro hardness tester in accordance with specifications outlined in ASTM E384-22 standard. The sample surface was first polished using a polishing wheel, then placed on the tester, the indenter was allowed to press on the surface for about 10 seconds, the hardness test was carried out twice for each sample, after which the resulting indent was analysed using the optical system and then the length of diagonals was used to determine the size of the impression.

2.7 X-RAY DIFFRACTION (XRD)

X-ray Diffraction analysis was carried out at Engineering Laboratory, Musa Yar'dua University Kaduna using Thermo scientific model: ARL'XTRA X-ray diffractometer with serial number 197492086. The intensity of the peaks was used to determine the phases present in the samples. The intensity was continuously recorded as the sample and detector rotate through their respective angles. The samples were polished to ensure smooth and defect free surface, they were then subjected to XRD analysis using Cu Kα radiation. Scanning was done in the 2θ range of 10-70° to get the austenite and ferrite peaks. The flow chart of the experimental procedure is shown in Figure 3.

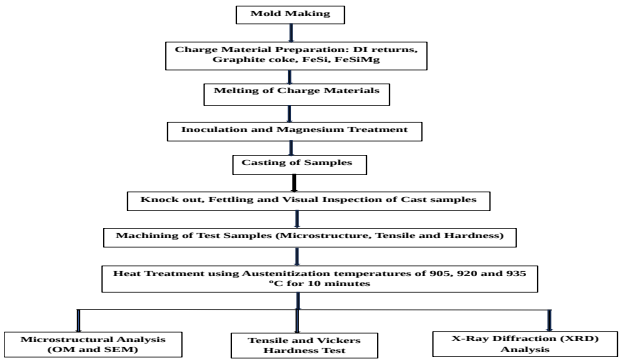

Fig. 3. Flow Chart of the Experimental Procedure

3 RESULTS AND DISCUSSION

3.1 CHEMICAL COMPOSITION OF THE CAST TWDI

The chemical composition of the cast TWDI sample is shown in Table 4, also the sample designation for easy identification is shown in Table 5. The cast samples chemical composition (Table 4) conforms to elemental composition as stipulated in ASTM A536 standard for nodular iron with a ferritic and pearlitic microstructure.

Table 4. Chemical analysis of cast TWDI samples

Elements	Fe	C	Si	Mn	S	Mg	Ni	Cu	Al
Wt. %	93.38	3.08	2.42	0.83	0.05	0.04	0.04	0.10	0.05

Table 5. Sample designations with their Austenitization temperatures

TWDI sample Number.	1	2	3	4	5	6	7	8
Austenitization temperature C	As cast, 3 mm	As cast, 4 mm	3 mm at 905	4 mm at 905	3 mm at 920	4 mm at 920	3 mm at 935	4 mm at 935

3.2 NODULE COUNT AND NODULARITY OF CAST SAMPLES

Using ASTM E407-15 and A247-19 specifications, the nodularity and nodule count of the as cast samples were estimated and are shown in Table 6. The nodule count values can be attributed to the fact that formation of carbides competes with graphite nucleation in the melt as during solidification of TWDIs, graphite's and carbides compete for carbon contained in molten iron (Davies 1996). These values remained unchanged during the heat treatment process for the two thicknesses adopted.

Table 6. Nodule count and Nodularity of sample

S/N	Sample No.	Nodularity (%)	Nodule Count in nodules/mm^2
1	Sample 1	89	566
2	Sample 2	85	543

© 2026 The Author(s). Published by Faculty of Engineering, Federal University Oye-Ekiti.
This is an open access article under the CC BY NC license. (https://creativecommons.org/licenses/by-nc/4.0/)

http://dx.doi.org/10.46792/fuoyejet.v11i3.1559 engineering.fuoye.edu.ng/journal

3.3 Optical Micrographs (OM) of Samples

The optical micrographs of 3- and 4-mm cast and heat-treated samples is shown in Figure 4a and b to Figure 7a to b. The optical micrographs of the etched samples for as cast 3- and 4-mm samples are shown in Figure 4a and Figure 4b respectively. The as cast microstructure showed carbide precipitates, which could be seen to nucleate alongside the ferrite/pearlite matrix, the pearlite phase was significantly larger in volume than the ferrite phase. Micrographs of the etched 3- and 4-mm samples that were austenitized at 905 °C are shown in Figure 5a and Figure 5b respectively. Also, those austenitized at 920 °C are shown in Figure 6a and Figure 6b, Figure 7a and Figure 7b shows that of those austenitized at 935 °C for 3- and 4-mm samples respectively. There was significant decrease in the carbide precipitates as the austenitizing temperature increased. The as cast etched samples had the highest volumes of carbide precipitates, followed by the samples austenitized at 905 °C. In fact, as the austenitization temperature increased, carbide precipitates decreased, this is due to the increased temperature which favoured more carbide dissolution. This is evident in Figure 6a, Figure 6b, Figure 7a and Figure 7b for samples 5, 6 ,7 and 8 respectively where the microstructures showed little or no carbide precipitates. This trend was also observed in Giacopini et al. (2003) where the researchers adopted increase in soaking time during annealing heat treatment to reduce and eliminate carbide precipitations. These carbide precipitates are undesirable in TWDIs as they lower mechanical properties by reducing the strength of the TWDI part. Samples 7 and 8 as shown in Figure 7a and Figure 7b gave the least carbide precipitates in their microstructure after their annealing treatment. At this juncture, it is important to mention, that no significant thickness effects were observed for the 3- and 4-mm samples, the two thicknesses showed similar microstructures.

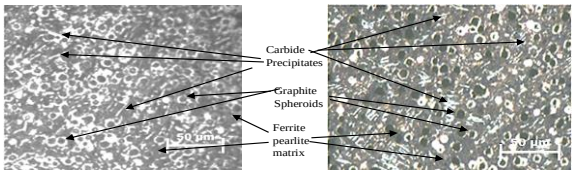

Fig. 4a. Sample 1 (As cast) Fig. 4b. Sample 2 (As cast)

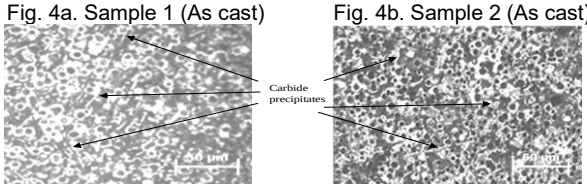

Fig. 5a. Sample 3 Fig. 5b. Sample 4

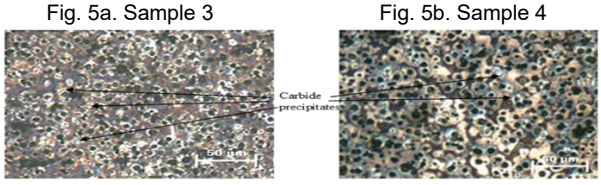

Fig. 6a. Sample 5 Fig. 6b. Sample 6

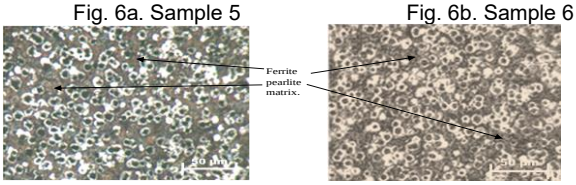

Fig. 7a. Sample 7 Fig. 7b. Sample 8

3.4 Scanning Electron Micrographs (SEM) of Samples

The SEM micrographs for samples 2, 4, 6 and 8 are shown in Figure 8 to Figure11 respectively. The SEM analysis was conducted on only the 4 mm thick samples. The SEM micrograph followed the same trend as that of their optical counterparts. The as cast SEM micrograph as seen in Figure 8 showed increased volumes of carbide precipitates in its microstructure whereas these reduced progressively with increase in austenitization temperature. No significant carbide precipitate was observed in the microstructure of sample 8 which was austenitized at 935 °C (Figure 11).

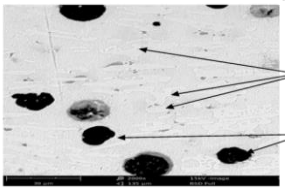

Fig. 8. Sample 2 (As Cast)

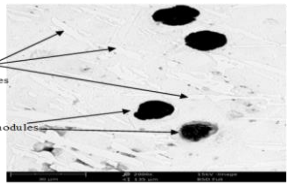

Fig. 9. Sample 4 (SEM)

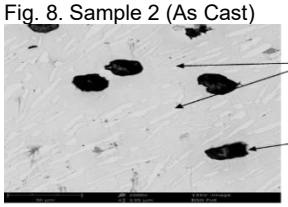

Fig. 10. Sample 6 (SEM)

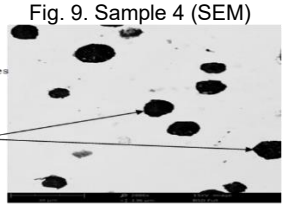

Fig. 11. Sample 8 (SEM)

3.5 Tensile Strength

The ultimate tensile strength chart for the samples is shown in Figure 12. There was slight reduction in UTS values from 578.5 MPa to 546 MPa for the as cast 3 mm sample to the 935 °C austenitized sample of same thickness, also the same trend was observed for the 4 mm sample where its strength reduced from 578 MPa to 553 MPa (Figure 12). This could be attributed mainly to the reduction of the pearlite phase in the as cast microstructure to a mixture of the ferrite and pearlite phases as austenitization temperature is increased during heat treatment, another contribution to this is the progressive increase in carbide dissolution as the austenitization temperature is increased. These two aforementioned factors contributed to the reduction of the UTS value as austenitization temperature was increased during heat treatment. This was seen in Fig. 4a and Fig. 4b for the as cast samples and also observed in Fig. 7a and Fig. 7b for samples austenitized at 935 °C. This slight reduction in UTS is in consonance with the UTS results observed in the study conducted in Akinribide et al. (2021). Also, in the study conducted in Dodo et al. (2023), where austempering holding times were investigated, longer holding times gave samples with lower UTS values.

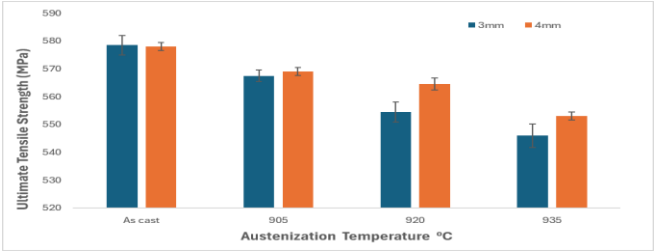

Fig. 12. Chart for UTS versus austenitization temperature

© 2026 The Author(s). Published by Faculty of Engineering, Federal University Oye-Ekiti.
This is an open access article under the CC BY NC license. (https://creativecommons.org/licenses/by-nc/4.0/)

http://dx.doi.org/10.46792/fuoyejet.v11i3.1559 engineering.fuoye.edu.ng/journal

3.6 Vickers Hardness

The chart for Vickers hardness value of the samples is shown in Figure 13. The hardness values (Figure 13) decreased with increase in austenitizing temperature; this can be attributed to the reduction of the carbide precipitates and pearlite phase as the annealing austenitization temperature increased. The as cast samples had the highest hardness values of 290.9 and 289.9 Hv for the 3- and 4-mm cast samples respectively as seen in Figure 13. There was a progressive reduction in Vickers hardness value as the annealing austenitization temperature was increased. Samples austenitized at 935 °C gave the lowest hardness values of 277.2 and 273.9 Hv for 3- and 4-mm samples respectively with the values of 905 °C and 920 °C being in between. The reduction in the carbide precipitates resulted from more carbides going into solution as the austenitization temperature increased. These results correlate with the phases as observed in the various microstructures.

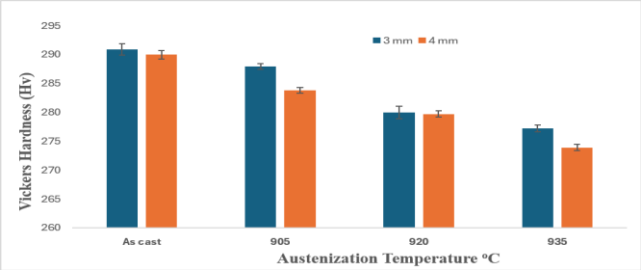

Fig. 13. Chart for Vickers hardness versus austenitization temperature

3.7 Percent Elongation/Ductility

The chart for percent elongation value of the samples is shown in Figure 14. The percent elongation chart (Figure 14) shows an increase in percent elongation as annealing austenitization temperature increased. This resulted from more carbide dissolution at higher temperatures and increase in volume of the ferrite phase from the initial as cast carbide content. Percent elongation values had a direct relationship with austenitization temperature. The highest percent elongation/ductility of 8.3 and 8.5 was observed for 3- and 4-mm samples austenitized at 935 °C. This trend correlates with the percent elongation/ductility results observed in the study conducted in Akinribide et al. (2021) where improved ductility level of the developed samples was observed.

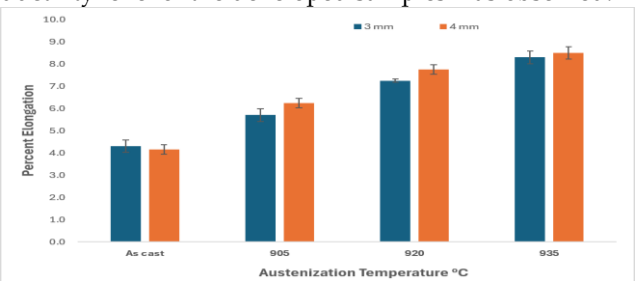

Fig. 14. Chart for percent elongation versus austenitization temperature

3.8 X-ray Diffraction (XRD) Analysis

The X-ray diffraction analysis was conducted for selected samples namely: A, B, C and D representing samples 1, 3, 5 and 7 (refer to Table 5) to study the phases present in 3 mm thick sample's microstructure. These patterns are shown in Figure 15. The XRD analysis patterns (Figure 15) indicated that TWDI samples are mainly composed of graphite nodules, eutectic carbides (Fe_3C), and pearlite/ferrite matrix which agrees with phases observed in the study of Sulamet-Ariobimo et al (2020). The pattern for sample 1 showed the presence of M_3C type carbide precipitate occurring at 2θ angle of 38° with high peak intensity. These M_3C carbides are the eutectic carbides called cementite (Fe_3C). This peak is also evident in sample 3, also in samples 5 and 7, though with much lower intensity. This lower intensity confirmed significant reduction of the carbide precipitates as annealing austenitization temperature was increased as seen in XRD patterns for 920 °C and 935 °C austenitized samples (samples 5 and 7). Iron carbide with peak at 2θ angle of 44° in (220) plane, BCC ferrite (α-Fe) and graphite peaks all at braggs angle of 44° are the main constituent observed in the as cast and 905 °C austenitized sample (samples 1 and 3). The cementite and ferrite peaks show that pearlite structure is present in the matrix of samples 1 and 3 as pearlite is made up of alpha-ferrite (α-Fe) and cementite (Fe_3C). Low-intensity BCC ferrite (α-Fe) peak in (200) plane at Bragg's angle of 66° was observed in all sample patterns. The peak exhibited in plane (100) at Bragg's angle of 42° for samples 1 and 3 show the presence of graphite, which shows that carbon is one of the main elements in TWDIs. These phases were also evident in the optical and SEM micrographs of the samples.

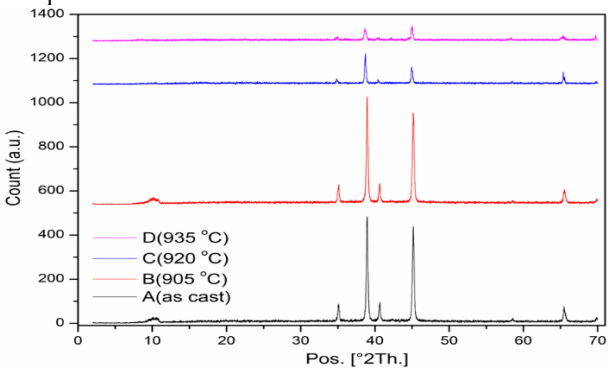

Fig. 15. XRD patterns for samples A, B, C and D

4 CONCLUSION

This study investigated annealing treatment austenitizing temperatures of as-cast TWDI samples containing large proportions of carbide precipitates in their microstructure. The results showed that samples 1 and 2 (as-cast 3 and 4 mm) exhibited mainly a pearlitic structure with reduced ductility and a moderate nodularity and nodule count ratings. The reduction/elimination of these carbide phases was achieved when higher austenitizing temperatures of 920 and 935 °C were adopted. Microstructure with reduced carbide precipitation and better mechanical properties were observed as austenitization temperature was increased. The annealing treatment conducted in this study using 935 °C austenitizing temperature has shown to be effective in reducing or eliminating carbide phases in cast TWDIs, consequently saving foundry cost by reduction of the amount of defective TWDI castings.

ACKNOWLEDGEMENT

The contribution of the laboratory staff in the Department of Metallurgical and Materials Engineering, Unilag and that of my project students that worked tirelessly to see to

© 2026 The Author(s). Published by Faculty of Engineering, Federal University Oye-Ekiti.
This is an open access article under the CC BY NC license. (https://creativecommons.org/licenses/by-nc/4.0/)

http://dx.doi.org/10.46792/fuoyejet.v11i3.1559 engineering.fuoye.edu.ng/journal

the completion of this research is greatly appreciated

REFERENCES

Adebayo, A. O., & Oyetunji, A. (2017). Production of ductile iron from waste sleeve scraps for automobile applications. Fuoye Journal of Engineering and Technology, 2 (1), 72-78. https://doi.org./10.46792/fuoyejet.v2i1.61

Akinribide, O. J., Olusunle, S. O. O., Akinwamide, S. O., Babalola, B. J., & Olubambi, P. A. (2021). Impact of heat treatment on mechanical and tribological behaviour of unalloyed and alloyed ductile iron. Journal of Materials Research and Technology, 14, 1809-1819. https://doi.org/10.1016/j.jmrt.2021.07.077

ASTM E2349 -19 Standard Practice for Safety Requirements in Metal Casting Operations. American Society for Testing and Materials (ASTM) International

ASTM E3 -11 (2017) Standard Guide for Preparation of Metallographic Specimen. American Society for Testing and Materials (ASTM) International

ASTM E407-15 Standard Practice for Microetching Metals and Alloys. American Society for Testing and Materials (ASTM) International.

ASTM A247-19 Standard Test Method for Evaluating the Microstructure of Graphite in Iron Castings. American Society for Testing and Materials (ASTM) International.

ASTM E8/E8M -16 Standard Test Methods for Tension Testing of Metallic Materials. American Society for Testing and Materials (ASTM) International

ASTM E384 -22 Standard Test Method for Knoop and Vickers Hardness of Materials. American Society for Testing and Materials (ASTM) International.

Berdin, C., Dong, M. J., & Prioul, C. (2001). Local approach of damage and Fracture toughness for nodular cast iron. *Engineering Fracture Mechanics,* 68 (9), 1107-1117. https://doi.org.10.1016/S0013-7944(01)00010-8

Bockus, S., Venckunas, A., & Zaldarys, G. (2008. Relation between section thickness, microstructure and mechanical properties of ductile iron castings [J]. *Materials Science (MEDZIAGOTYRA),* 14 (2), 115. https://matsc.ktu.lt/index.php/MatSc/article/view/26242

Caldera, M., Chapetti, M., Massone, J. M., & Sikora, J. M. (2007). Influence of nodule count on the fatigue properties of ferritic thin wall ductile iron. *Materials Science and Engineering*, 23 (8), 1001-1004. https://doi.org.10.1179/174328407X185910

Choi, J. H., Oh, J. K., Choi, C. O., Kim, J. K., & Rohatgi, P. K. (2004). Effect of rare earth elements on microstructure formation and mechanical properties of thin wall ductile iron castings. *Journal of Material Science and Engineering,* A (383), 323-333. https://doi.org.10.1016/j.msea.2004.04.060

Davis, J. R. (1996). ASM Specialty Handbook Cast Irons. ASM International, *The Material Information Society*. 65-68.

Dodo, R. M., Musa, Z., Bello, K. A., Abdullahi, U., & Okoh, E. (2023). Time depended austempering of high carbon steel using epoxidized cotton seed oil. *Fuoye Journal of Engineering and Technology,* 8 (1), 96-99. https://doi.org./10.46792/fuoyejet.v8i1.944

Fraś, E., Górny, M., & Kapturkiewicz, W. (2013). Thin Wall Ductile Iron Castings: Technological Aspects. *Achieves of Foundry Engineering*, 13 (1), 23-28. https://doi.org./10.2478/afe-2013-0005

Giacopini, A., Boeri, R. E., & Sikora, J. A. (2003). Carbide dissolution in thin wall ductile iron. *Materials Science and Technology*, 19 (12), 1755-1760. https://doi.org.10.1179/026708303225009445

Górny, M., & Tyrała, E. (2013). Effect of cooling rate on microstructure and mechanical properties of thin-walled ductile iron castings. *Journal. of Materials Engineering and Performance.* 22 (1), 300–305. https://doi.org/10.1007/s11665-012-0233-0

Mourad, M. M., El-Hadad, S., Ibrahim, M. M., & Nofal, A. A. (2015). Effect of processing parameters on the mechanical properties of heavy section ductile iron. *Journal of Metallurgy*, 9, 1-11. https://doi.org.10.1155/2015/931535

Ochulor, E. F., Adeosun, S. O., Ekeleme, J. U., Ugboaja, J. O., & Nnaji, R. N. (2019). Carbide characterization in single and double step inoculated thin wall ductile iron. *Unilag Journal of Medicine, Science and Technology*, 6 (1), 15-32. https://ujmst.unilag.edu.ng/article/view/361

Ochulor, E. F., Amuda, M.O.H., Adeosun, S. O., & Balogun, S. A. (2018). Potential of green sand rice husk ash mould as carbide deactivator in thin wall ductile iron. *The West Indian Journal of Engineering (WIJE),* 41 (1), 4-12. https://journals.sta.uwi.edu/ojs/index.php/wije/article/view/9182

Riebisch, M., Pustal, B., & Bu¨hrig-Polaczek, A. (2020). Influence of carbide promoting elements on the microstructure of high silicon ductile iron. *International Journal of Metalcasting*, 14 (4), 1152-1161. https://doi.org.10.1007/s40962-020-00442-1

Sheikh, M. A. (2008). Production of carbide-free thin ductile iron castings. *Journal of University of Science and Technology Beijing, Mineral, Metallurgy, Material*, 15 (5), 552-555. https://doi.org.10.1016/S1005-8850(08)60103-6

Shinde, V. D., Ravi, B., & Narasimhan, K. (2012). Solidification behaviour and mechanical properties of ductile iron castings with varying thickness. *International Journal of Cast Metal Research.* 25 (6), 364-373. https://doi.org/10.1179/1743133612Y.0000000024.

Sulamet-Ariobimo, R. D., Santoso, J. R., Fadhlan, M., Yasin, T., Mujalis, Y., & Oktaviano, Y. (2020). The effects of austenitizing process to mechanical properties of thin wall ductile iron connecting rod. Paper presented at the 1st International Seminar on Advances in Metallurgy and Materials, Jakarta, Indonesia, AIP Conference Proceedings 2262 (1), 060006. https://doi.org/10.1063/5.0016141.

© 2026 The Author(s). Published by Faculty of Engineering, Federal University Oye-Ekiti.
This is an open access article under the CC BY NC license. (https://creativecommons.org/licenses/by-nc/4.0/)